PERFORMANCE ANALYSIS OF RIS-ASSISTED SSK MODULATION

PROJECT REPORT

Submitted by

Vaishali Upperwal - 214102013

Submitted in partial fulfilment of the requirements for the Degree of Master of Technology in Communication Engineering

Under The Guidance of

Dr. Manoj B. R.
Assistant Professor

Department of Electronics and Electrical Engineering

Indian Institute of Technology,Guwahati
Assam-781039

November 2022

ACKNOWLEDGEMENT

I want to sincerely thank my supervisor **Dr. Manoj B. R. , Assistant Professor,** Department of Electronics and Electrical Engineering for all of his assistance and encouragement during this project. This dissertation would not have been possible without his suggestions and carefully thought-out method of evaluation. The freedom, regular discussion and the relaxed learning environment he provided kept me constantly engaged with my research work.

I take immense pleasure in expressing my sincere heartfelt thanks to all the faculty members of EEE Department for the knowledge they have imparted.

Last but not least, I want to express my gratitude to this university, PhD students of the EEE department, my family, and my friends for giving me the resources I needed to finish this project successfully.

ABSTRACT

Reconfigurable Intelligent Surfaces (RIS) are envisioned as a new wireless technology that might enable radio signals' dynamic and goal-oriented regulation between a transmitter and a receiver, effectively turning the wireless environment into a service. RIS can dynamically alter wireless channels to increase communication effectiveness by carefully controlling the reflected signal via a sizable amount of affordable passively contemplating devices. RIS has recently emerged as a viable new paradigm for developing intelligent and reconfigurable wireless channels or radio propagation environments for 5G and 6G wireless communication systems. This provides a novel approach to the wireless channel fading impairment and interference problem and may significantly increase the capacity and reliability of wireless communication. When using Spac Keyinge Shift, the single transmit antenna is activated each time and detail is implicitly conveyed using the operational transmit antenna index. By leveraging the transmit antenna indices, an SSK technique based on RIS is created to prevent inter- channel interference and avoids the need of inter-antenna synchronization while offering an incredibly dependable and energy-efficient transmission. [1] Due to its exceptionally low error rates and exceptionally high energy efficiency, the RIS-based SSK scheme significantly surpasses the reference systems. Furthermore, the RIS-based SSK system may do away with the requirement for complex coding techniques to ensure reliable communications because it can be employed effectively even in sites with extremely low SNR. Reflection Phase Modulation (RPM) constellation controls the phase changes caused by reflecting elements. We investigated a unique RIS-SSK-RPM scheme that fully uses the benefits of both a "Re-configurable Intelligent Surfaces" and "Spac Keyinge Shift". The suggested method increases the system's Spectral Efficiency (SE) and communication link dependability by directly sending the data via reflection phase shift and reflecting the incoming Radio Frequency signal. To evaluate the unified tight upper bound expression of average bit error rate (ABER) for the given system, a closed-form expression of average pairwise error probability (PEP) over fading channels has also been created under the assumption of Maximum Likelihood (ML) detection.

CONTENTS

LIST OF FIGURES

CHAPTER 1
INTRODUCTION

1.1 Wireless Communication

The transfer of data over a significant distance without the use of enhanced electrical conductors or ”wires” is referred to as wireless communication. In the relatively limited history of **Wireless Communication**, a lot has been accomplished. In the past, numerous wireless access technology evolutionary paths have all resulted to the same outcome: efficiency and performance are crucial in a high-mobility scenario. Mobile phones' first generation (1 G) offered only the most fundamental voice services; the second generation (2G) improved capacity and coverage. The third generation (3G) comes next, which requires faster data speeds to unleash the doors to a truly ”mobile broadband” experience. The fourth generation (4G) will further achieve this. Both mobile technology and user numbers in the wireless industry have increased rapidly in recent years. Wireless communication systems have evolved into a fundamental component of contemporary communication networks as a primary means of exchanging and transmitting information.

In order to provide us with great real-world wireless communication, the fifth wireless mobile multimedia internet networks require unfettered wireless connection. Wireless World Wide Web (WWWW). The 4G technology will be upgraded to 5G, which is constructed on top of it. Throughout this procedure, there are two distinct sorts of issues that need to be fixed. The first is expanded coverage, and the second is unrestricted switching between technologies. Global coverage for 6th generation (6G) wireless mobile communication networks will be provided via satellites.

Mobile wireless technologies have advanced and changed technologically over numerous generations, from 1G to 4G. Future and existing cellular generations, including 5G, 6G, and 7G, are being introduced. Over the past few decades, mobile wireless communication networks have seen a significant development. Each generation distinguishes from the previous one in aspects of norms, abilities, techniques, and distinctive qualities.[2]

1.2 Reconfigurable Intelligent Surfaces (RIS)

Reconfigurable intelligent surfaces technology allows it to design how radio signals spread over wireless networks. RIS can dynamically switch wireless channels to increase the effectiveness of communication, to carefully adjusting the reflected signal via many inexpensive passive reflecting devices. As a consequence of this, it is projected that the newly developed RIS-aided hybrid wireless network, which is comprised of both active and passive components, would be very promising in the future in terms of attaining sustained capacity increase

in a cost-effective manner.

In spite of the fact that RIS can be thought of as a re-configurable meta-surface, it advances the systems and applications of meta-surface by influencing electromagnetic (EM) waves to the cutting-edge of wireless communication as an inventive enabling factor for an intelligent and re-configurable propagation environment. These traditional uses of meta-surface include invisibility cloaking, imaging, radar sensing, and holograms.

Moreover, RIS is flexibly located in the network to assist in modifying the wireless communication channel leveraging intelligent reflection as opposed to the traditional reflect array, which places a passive mirror or lens with fixed or re-configurable beam patterns in the vicinity of the wireless receiver to save the active antennas/RF chains. Despite its enormous promise, RIS must overcome new obstacles before it can be effectively used in wireless networks. These challenges come in the form of optimizations for reflection and channel estimations, as well as deployment from the point of view of communication design.

1.2.1 System Model

For illustrative purposes, we will examine the simplest point-to-point communication system, in which communication between a transmitter and its intended recipient is facilitated by the deployment of a RIS consisting of N passive reflecting pieces on a flat surface. For illustration, we will consider a single antenna at both the transmitter and receiver, as well as a system with a restricted band and a defined carrier frequency. The carrier frequency is denoted by the phrase fc, while the system bandwidth is denoted by the term B, both of which are measured in hertz (Hz), with B being less than or equal to fc.

The comparable complex-valued base-band transmit signal is denoted by $x(t)$. We first concentrate on the signal transmission from the transmitting device to the receiving device through a RIS reflecting component, n, having a value $n = 1, \ldots, N$. The analogous complex base-band channel coefficient to the RIS element from the transmitter n is denoted by $\alpha_{1,n}e^{-j\gamma_{1,n}}$, where $\alpha_{1,n}$ and $\gamma_{1,n}$ stand for the frequency-flat channel's amplitude attenuation and phase shift, respectively. So n is impinged by the pass-band signal supplied by:

$$y_{i,n}(t) = \mathrm{Re}\left\{\alpha_{1,n}e^{-j\gamma_{1,n}}x(t)e^{j2\pi f_c t}\right\} \tag{1.1}$$

It is noted that the output signal of n in the base-band signal model is obtained by multiplying the input signal with a complex reflection coefficient $\beta_n e^{j\theta_n}$, where, $\theta_n \in [0, 2\pi]$ and $\beta_n \in [0, 1]$. The signal that is reflected goes via an identical or equivalent frequency-flat channel that is narrow-band. described by $\alpha_{2,n}e^{-j\gamma_{2,n}}$ before reaching the receiver from RIS element n. Next, the pass-band signal received by the receiver after being reflected by RIS element n is written as

$$y_{r,n}(t) = \mathrm{Re}\left\{\left[\alpha_{1,n}e^{-j\gamma_{1,n}}\beta_n e^{j\gamma_n}\alpha_{2,n}e^{-j\gamma_{2,n}}x(t)\right]e^{j2\pi f_c t}\right\} \tag{1.2}$$

Thus, the cascaded channel via RIS element n from the broadcaster to the receiver has been modelled. Given below is the base-band signal model for eq. 1.2. And, let $h^*_{r,n} = \alpha_{1,n}e^{-j\gamma_{1,n}}$ and $g_n = \alpha_{2,n}e^{-j\gamma_{2,n}}$.

$$y_n(t) = \beta_n e^{j\theta_n}h^*_{r,n}g_n x(t) \tag{1.3}$$

Three terms are multiplied to create the RIS reflected channel,including, the transmitter-to-element n channel, the element n-to-receiver channel, and the RIS reflection,as can be seen from eq. 1.3.

Provided that each RIS element's received signal can be characterized as a superposition of its own reflected signal, the base-band signal model that accounts for all N RIS elements is given by:

$$y(t) = \left(\sum_{n=1}^{N} \beta_n e^{j\theta_n} h_{r,n}^{*} g_n \right) x(t) = \boldsymbol{h}_r^H \Theta \boldsymbol{g} x(t) \tag{1.4}$$

$\theta = \text{diag}\left(\beta_1 e^{j\theta_1}, \beta_2 e^{j\theta_2}, \ldots, \beta_N e^{j\theta_N}\right)$ is the NxN diagonal complex reflecting matrix, $h_r^H = \left[h_{r,1}^{*}, h_{r_{1,2},\ldots}^{*}, h_{r,N}^{*}\right]$ and $g = [g_1, g_2, \ldots, g_N]^{\top}$ are the channel coefficients which basically rely on path loss due to distance, large-scale shadowing, and small-scale multi-path fading. Because each RIS element reflects the signal independently and there is no signal coupling or joint processing over the RIS elements, the RIS with N elements essentially performs a linear mapping from the incident signal vector to a reflected signal vector by a NxN diagonal complex reflecting matrix.[3]

(i) Channel Estimation

Accurate channel state information (CSI) must be obtained, which is difficult, realistically, to fully realize the many performance advantages brought on by RIS. Another difficulty in RIS channel estimation arises from its low-cost reflecting elements, which have no active RF chains and cannot transmit pilot or training signals to facilitate channel estimation. This is in sharp contrast to the active BSs in conventional wireless systems. This is in addition to the significantly more RIS-induced channel coefficients than the traditional system without RIS. Depending on whether it is mounted with sensing devices (receive RF chains) or not, there are two basic methodologies for RIS channel estimation based on two different configurations, referred to as semi-passive RIS and (completely) passive RIS [4].

The new RIS technology is a promising facilitator for an intelligent and adaptable wireless communication environment. RIS-enabled wireless communication has caused a fundamental paradigm shift in wireless system design from the conventional one with only active components to a new hybrid architecture encompassing both active and passive components that co-work intelligently. Despite the fact that research on RIS-aided wireless communication is still in its early stages, there are a number of new challenges and potential directions of future RIS-aided wireless networks, ranging from theoretical RIS signal and channel modeling to actual RIS beamforming design, channel estimation, and deployment.

1.3 Space Shift Keying Modulation (SSK)

More than two antennas are used in the space modulation system to transmit and signal the information bits. For binary signalling, such as in the "Binary Phase Shift Keying" BPSK or "Binary Phase Shift Keying" binary-FSK modulation on wireless fading channels, two antennas are typically used. "Space Shift Keying" SSK is the name of the new space modulation method. The SSK's fundamental tenet is based on the distinct multi-path properties of various antennas on a wireless fading channel. As a result, the receiver may discern the sent information packets using the diverse received signals from various antennas, leading to a simple and affordable

receiver structure. Demodulation and detection of SSK signalling will be simpler to accomplish as a result.

In this context, binary signalling with a single receiver antenna is taken into consideration in wireless fading channels with Rayleigh or Rician distributions. At the transmitter side, different numbers of antennas transmit binary information. Only the first antenna sends a tailored signal if the information bit 0 is to be conveyed. On the other hand, if information bit 1 is to be communicated, both the first and second antennas provide the intended signal. Maximum likelihood (ML) detector is used at the receiver side to estimate the information data bits.

The SSK modulation scheme can also be combined with more established modulation techniques, such as PSK or FSK, to create the SSK-BPSK or SSK-FSK modulations, which improve the data rate.

(i) SSK Signal Modelling

Consider the signalling on a Rayleigh or Rice fading channel that is slow non-frequency selective. The transmitted signal vector of the antenna elements with the SSK modulation technique is represented by;

$$\mathbf{s}_n(t) = \begin{bmatrix} s_{n1}(t) & s_{n2}(t) \end{bmatrix}' \; n = 0 \text{ or } 1 \tag{1.5}$$

for $0 \leq t \leq T_b$, where $s_{nl}(t)$ is the transmitted signal of the lth antenna, T_b is the transmission duration. For $0 \leq t \leq T_b$, the binary signals of the two antennas given in eq (1.5) are characterized by

$$s_{n1}(t) = \sqrt{Z}\cos 2\omega_c t \tag{1.6}$$

for $n = 0, 1$ and

$$s_{n2}(t) = \begin{cases} 0 & if\ n = 0 \\ \sqrt{Z}\cos 2\omega_c t & if\ n\ =\ 1 \end{cases} \tag{1.7}$$

where Z represents the overall transmission power and each antenna consumes half of Z. In accordance with the SSK modulation signal model discussed above, different numbers of antennas carry the digital information before it is broadcast. The ideal receiver is designed in the following context for SSK demodulation and detection.

The fading factor α_l is taken to have a complex Gaussian distribution with a mean of b_l and a variance of ω_l for a Rayleigh or Rice channel that fades slowly. As a result, the received signal for $0 \leq t \leq T_b$ in complex form at the receiver is delivered by

$$p(t) = \begin{cases} \alpha_1\sqrt{Z}e^{j\omega_c t} + w(t) & if\ n = 0 \\ \alpha_1\sqrt{Z}e^{j\omega_c t} + \alpha_2 e^{j\omega_c t} + w(t) & if\ n\ =\ 1 \end{cases} \tag{1.8}$$

where $w(t)$ is the additive channel noise, which has a complex Gaussian distribution with zero mean, and α_l, for $l = 1, 2$ denotes the complex fading factor from wth transmit antenna to the receiver antenna. In eq (1.8), we assume that α_1 and α_2 are independent and that $\frac{N_o}{2}$ is the power spectrum density of the quadrature and

in-phase parts of w(t).

The received signal is identified by after being down-converted into its equivalent base-band form eq (1.7):

$$u = \begin{cases} \alpha_1\sqrt{Z} + \upsilon & if\ n = 0 \\ \alpha_1\sqrt{Z} + \alpha_2\sqrt{P} + \upsilon & if\ n\ =\ 1 \end{cases} \tag{1.9}$$

where the complex fading factors α_l for $l = 1, 2$ have to be approximated at the receiver for the detection of information bits, and u has a Gaussian distribution with 0 mean and variance N_o. When the information data bit n has been delivered, the signal u has been received has a complex Gaussian distribution with mean μ_n and variance σ_n^2, where $\mu_0 = \sqrt{Z}b_1, \mu_1 = \sqrt{Z}\left(b_1 + b_2\right), \sigma_0^2 = Z\Omega_1 + N_0$ and $\sigma_1^2 = Z\left(\Omega_1 + \Omega_2\right) + N_0$

The created SSK scheme can also be employed with Quadrature Phase Shift Keying (QPSK) and other other digital modulation schemes. To create broadcast variety and improve reception, more than two antennas might be employed. Besides, by adding additional transmit antennas, the suggested space modulation system can also be expanded to the scenario of a higher amount of modulation, similar to M-ary signalling. [5]

CHAPTER 2
LITERATURE REVIEW

2.1 Intelligent Reflecting Surface

The ”Sixth-Generation” 6G wireless network aspires to higher standards than the ”Fifth-Generation” 5G network, including exceptionally high data rates, energy efficiency, connectivity, and diversification, as well as extremely high consistency and quick response. Although the 5G wireless network is still being deployed throughout the world, research into the future beyond 5G has received strong support from both academia and industry. [6]. These needs might not be fully met with the current technology developments for 5G services such as increased mobile massive machine-type communication (MMTC), ultra-reliable and low latency communication (URLLC), and broadband (m-MTC) which primarily consist some factors such as [7] [8]:

a. Deploying an increasing number of active nodes, such as base stations (BS), access points (AP), relays and distributed antennas, to reduce the distance between communication nodes in order to increase network coverage and capacity; this, however, results in higher energy consumption, deployment or maintenance costs, as well as more severe and complex network interference issues.

b. Utilizing many more antennas at the BS, AP, and relays to maximize the large Massive Multiple-Input-Multiple-Output (M-MIMO) benefits, demands more complicated signal processing and higher hardware and energy costs.

c. Moving to higher frequency bands, like millimeter wave (mm-wave) and even terahertz (tHz) frequencies, in order to take advantage of their expansive bandwidth, unavoidably results in the installation of additional antennas and the implementation of further active nodes on them in order to compensate their greater propagation loss over distance.

Given the aforementioned problems and constraints, it is crucial to develop new and innovative technologies that will enable future wireless networks to expand their capacity while maintaining low cost, low complexity, and low energy consumption.Traditional methods of addressing this problem either use different modulation, coding, and diversity techniques to compensate for the channel fading, or use adaptive power control and beamforming techniques to adapt to it. They are still unable to overcome the biggest obstacle standing in the way of establishing high-capacity and ultra-reliable wireless communications since they not only require more overhead but also have less influence over the wireless channels, which are mostly random.
As a result of the foregoing, **Re-configurable Intelligent Surface (RIS)** has recently emerged as a promising

new paradigm to provide intelligent and re-configurable wireless channels or radio propagation environments for 5G/6G wireless communication systems. IRS is a planar surface comprising of numerous passive reflecting components, each of which can independently cause the incident signal to vary in amplitude and/or phase.[9] RISs can be implemented in a variety of ways, such as vast arrays of cheap antennas that are typically placed half the wavelength apart and planar or conformal big surfaces based on meta-materials, whose scattering elements have sizes and inter-distances much lower than the wavelength. RISs require the most scattering parts compared to other transmission systems, such as multi-antenna transmitters and relays, yet each one only needs to be supported by a small number of cheap components. Furthermore, power amplifiers are typically unnecessary.

The signal propagation/wireless channels between transmitters and receivers can be flexibly reconfigured to achieve desired realizations and/or distributions by densely deploying RISs in wireless networks and strategically coordinating their reflections. This offers a new way to tackle the wireless channel fading impairment and interference issue and could potentially achieve a quantum leap improvement for wireless communication capacity and reliability.

In wireless channel reconfiguration, RIS can perform a number of appealing tasks, such as establishing a virtual line-of-sight (LoS) link to avoid obstacles between transceivers via smart reflection, adding additional signal paths in the desired direction to improve the channel rank condition, improving the channel statistics/distribution by, for example, switching from Rayleigh/fast fading to Rician or slow fading for ultra-high reliability, suppressing or nulling co-channel interference, and more as shown in the attached figures: [10]

Advantages:

a. In contrast to conventional active antenna arrays or the recently suggested active surfaces, it can be implemented and operated with orders-of-magnitude lower hardware and energy costs because its reflecting elements (such as low-cost printed dipoles) merely passively reflect the impinging signals.

b. IRS operates in full-duplex (FD) mode and is free of any antenna noise amplification and self-interference in comparison to more conventional active relays, such as half-duplex (HD) relays that have low spectral efficiency and FD relays that require complex techniques for self-interference cancellation.

c. For deployment or replacement, IRS is often low profile, lightweight, and conformal in geometry, making it simple to mount to and remove from environment objects.

d. IRS is an auxiliary device that can be seamlessly integrated into wireless networks, giving it a lot of flexibility and compatibility with current wireless systems (e.g., cellular or WiFi).

Disadvantages:

a. To achieve cooperative signal focusing and/or interference cancellation in its immediate vicinity, the passive reflections of all reflecting elements at each IRS need to be properly configured. In the meantime, the IRS passive reflections must also be jointly designed with the BSs'/users' transmissions in order to

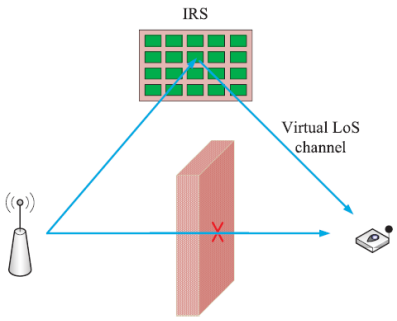

(a) IRS for extending coverage

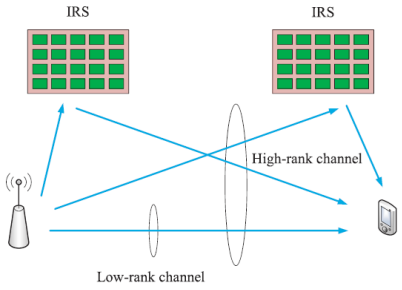

(b) IRS to improve the state of the channel rank

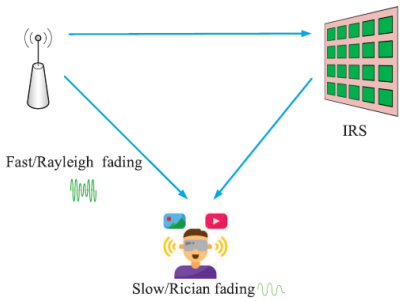

(c) Channel statistics refinement using RIS

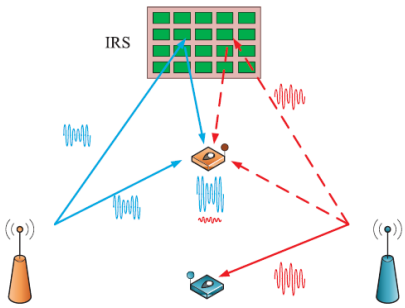

(d) Interference suppression technology

Figure 2.1: IRS's primary wireless channel reconfiguration functions.

optimise their end-to-end communications over the reconfigured wireless channels by RISs. This is necessary to serve all users in the network regardless of whether there is any associated IRS nearby each user.

b. Since IRS typically lacks RF chains, acquiring the channel state information (CSI) required for the aforementioned IRS reflection optimization between IRS and its serving BSs/users becomes a challenging task in practise, especially given that IRS typically has a lot of reflecting elements and thus associated channel coefficients to be estimated.

c. Since IRS typically lacks RF chains, acquiring the channel state information (CSI) required for the aforementioned IRS reflection optimization between IRS and its serving BSs/users becomes a challenging task in practise, especially given that IRS typically has a lot of reflecting elements and thus associated channel coefficients to be estimated.

2.2 Space Shift Keying Modulation

Wireless communication systems with many antennas enable next-generation communication features like higher data speeds, reliability, spectrum efficiency, and extensive coverage with unbroken service. Numerous Input MIMO communications offers potential methods that can be categorized into three categories: precoding, diversity coding, and spatial multiplexing (S-MUX). MIMO evaluation began with the Spatial Multiplexing technique and boosted transmission rates all the way up to multiple transmitting antennas. For the purpose of increasing the capacity of Multiple Input Multiple Output systems, this technique is used which makes use of the TA index to send more data bits. In order to increase the data flow, SM expands and utilizes the traditional constellation diagram by including a third dimension. These extra data bits are transmitted using the SM scheme's array index of TA.

Encoding is crucial in S-MUX (Spatial multiplexing) because the Rx must be able to recognize and decode the data sent on each wireless channel in order to retrieve the data bits from the originally transmitted source signal. Here, a group of symbols are transmitted concurrently through all antennas during a time slot without being duplicated or conjugated in the following time slot. As a result, the transmitter diversity gain was impaired in the plan. Additionally, antenna synchronization and spacing are needed. The complexity and Inter Channel Interference (ICI) at the Rx end would also increase as more and more transmit antennas were added to S-MUX in order to double the amount of broadcast bits. [11]

It has only been the last four or five years that SM-MIMO has attracted the attention of many researchers. Up until 2008, SM-MIMO research was conducted independently by researchers all over the world. The "space modulation" principle, commonly known as space shift keying(SSK), was first presented in 2001. SSK, or space shift keying, was developed to lessen the difficulty of detection. Only 4 antennas total—2 for transmission and 2 for reception—have been used in this arrangement. Depending on the data transmission antenna chosen, a single bit sign is conveyed. Bits '0' and '1' must be sent by the first antenna alone and by both antennas, respectively. As a result, the transmitter sends one piece of information at a time. This method offers a 1-bpcu data rate, and larger data rates were made possible by using more antennas and higher order signal modulations as QPSK and FSK. SSK, which uses an antenna selection technique, is thus the fundamental concept of SM. Out of the total of four antennas, only one active antenna is used in this multiplexing technique.

The receiver detects the transmit antenna on uncorrelated fading channel with perfect channel information. One bit in transmitting symbol cries parity information. So, it improves the signal to noise ratio (SNR) by 2.5 dB, nearly doubles the signal power as it seen with 8-PSK transmission without parity and inter channel interference (ICI) is avoided because one active antenna is transmitting in a symbol period. The capacity is directly proportional to number of antennas but not concentrated on RF chains reduction.[7]

Spatial and temporal diversity is provided by Alamouti [2 X 2] Space Time Code (STC). According to STC,

data is repeatedly sent as symbols through various antennas (space domain) and instants. Due to spatial and time diversity, these systems are reliable, although synchronization is necessary when multiple antennas are sending and receiving at once. However, compared to single antenna transmission, the transmission rate is unchanged. Later, Orthogonal Space Time Block Codes (OSTBC's) offered greater transmission speeds in addition to diversity gain. All of these techniques have increasing detection complexity as the number of antennas increases. Different strategies were suggested to reduce the Orthogonal Space Time Block Code's estimation complexity. Additionally, each antenna in these systems requires its own RF chain. As a result, power consumption rises roughly from 40 to 80 percentages in accordance with RF chains. [12]

SM-MIMO (Selective Antenna Transmission Systems) are essentially addressed as a means of avoiding those issues. Instead of all antennas transmitting concurrently, only one or a small number of them are active throughout each symbol period. These methods drastically reduce the complexity of the receiver's estimator, use less power because they only need one or fewer RF chains, and do away with inter-channel interference (ICI). An ideal maximum likelihood (ML) detector for SM-MIMO demonstrates that when one chosen antenna transmits symbol throughout a symbol period, complexity of ML detector grows exponentially and avoids ICI. [13]

2.3 RIS Assisted SSK Scheme

The Re-configurable Intelligent Surface (RIS)-based transmission concept, which does not require a dedicated energy source for radio frequency (RF) processing, decoding, encoding, or re-transmission, and instead uses a large number of small, inexpensive, and passive elements on a RIS to only reflect the incident signal with an adjustable phase shift, is completely different from existing MIMO, beam-forming, amplify-and-forward relaying, and back-scatter communication paradigms. In keeping with the definition of software-defined radio, which is defined as "radio in which some or all of the physical layer functions are software defined. In other words, they can be referred to as SDS since the reflection properties of these intelligent surfaces, walls, and arrays in the physical layer can be changed by software.
One of the early research proposes transmission through intelligent walls by using active frequency-selective surfaces to regulate the signal coverage.[14] As a promising alternative to beam forming techniques, which call for numerous antennas to focus the sent or received signals, smart reflect-arrays with passive reflector elements are offered. Additionally, it has been shown that reflect-arrays can be effectively used to shift the phase of incoming signals during smart reflection without buffering or processing them. The received signal quality can also be improved by adjusting the phase shift of each reflector element on the reflect-array.[15] Since RISs don't need transmit RF chains because their components are passive, they are much less expensive than active antennas for the AF relay. RIS-assisted communications stand out as an interesting and beneficial field of study for technologies beyond 5G because of all these advantages.

The promise of recent innovations like Index Modulation (IM) and THz communications for 5G and beyond is being ruthlessly explored by researchers. The growing IM idea, which has recently gained widespread

acceptance in academia and industry, employs the indices of the available transmit entities to transmit extra information bits in situations with abundant scattering. This is one of these unique techniques. For instance, the spatial modulation (SM) approach, which is based on IM, uses the index of a transmitter antenna that has been engaged to send additional information. Due to its special characteristic, SM is able to efficiently balance spectrum and energy efficiency. In addition, it resolves synchronization issues while eliminating any inter-channel interference at the receiver (Rx). [16]

A space shift keying (SSK) technique based on RIS is developed in order to avoid synchronization and interference issues by utilizing the Tx antenna indices in addition to provide an extremely reliable and energy-efficient transmission. The RIS-based SSK scheme clearly outperforms the reference designs thanks to its extremely low error rates and unusually high energy efficiency. Additionally, since the RIS-based SSK scheme may be used successfully even in extremely low SNR locations, it may also eliminate the need for complicated coding techniques to enable reliable communications. [17]

CHAPTER 3
System Model and Performance Analysis

3.1 Motivation and Problem Introduction

We demonstrate a ”Space Shift Keying” (SSK) modulation and a ”Reflection Phase Modulation” (RPM) scheme made possible by reconfigurable intelligent surfaces (RIS), which incorporate their own data into the reflection phase shift of the reflected radio frequency (RF) signal. In order to transfer the information bits from the infringing SSK modulated radio frequency (RF) signal coming from an Access Point (AP) to the receiver, RIS sends it with a discontinuous phase shift (Rx). To be more specific, the RIS here simultaneously does two tasks: first, it embeds the information bits in the phase shift and then reflects the impinging RF signal with a discrete phase shift. In order to conduct joint detection for the Reflection Phase Modulation (RPM) and SSK symbols, we will employ a maximum likelihood detector. We also provide a unified analytical framework for the theoretical analysis of this system's average bit error rate (ABER), diversity, and ergodic capacity.

In order to combat the fading effect of the propagation medium, reconfiguration intelligent surface (RIS), a new technology, is being developed for wireless communication standards beyond 5G. To improve the spectral efficiency (SE) of the communication system, we here present a RIS-assisted SSK and reflection phase modulation (RPM) technique known as the RIS-SSK-RPM scheme. In this system, the RIS transmits the impinging SSK-modulated radio frequency (RF) signal from the access point (AP) to the receiver with a discontinuous phase shift that delivers its information bits..[18]

3.2 System Model

In this system, a RIS with N reflecting elements is placed in the propagation medium to reflect the impinging wave with a distinct phase shift. This is known as a RIS-assisted ”Multiple-Input Multiple-Output” MIMO system. We presum that the Nt and Nr antennas are used to construct the access point (AP) and receiver (Rx), respectively. Given that the received signal's power is inversely correlated with the square of the number of reflecting components. The signal power received via direct link is negligible for large values of N. As a result, we don't take the direct connection into account here. The RIS controller also has sensors that collect environmental information like temperature and humidity. The sensed data is cleverly encoded into a reflection phase shift by the controller. The phase shifts brought on by reflecting elements are controlled by the RPM (unit-norm phase shift keying (PSK)) constellation. More specifically, the RIS reflects the AP signal to the

Rx while explicitly transmitting its data using M-ary RPM symbols. Through the use of a single antenna and Nt-ary SSK modulation, AP sends its data over the air.

Hence, x = a_i, where a_i is the ith column of the NtxNt identity matrix, can be used to define transmission vector for space shift keying modulation with active transmit antenna, where i = 1,2,.,Nt. $\{\theta_1, \theta_2, \ldots \theta_M\}$ is the representation of the M-ary RPM constellation's distinct phases and the value of θ_m at m = 1,2,...,M is given as $\theta_m = \frac{2\pi(m-1)}{M}$, $H \in C^{N_t \times N}$ and $G \in C^{N_r \times N}$ are the Access Point -to-RIS and RIS-to-Receiver links' respective channel gain matrices and $\theta = \text{diag}\left(e^{j\phi_1}, e^{j\phi_2}, \ldots, e^{j\phi_N}\right)$, which represents the RIS's reflection phase matrix.

3.3 Signal Model

The RIS concurrently reflects the wave from the AP that is impinging on it and incorporate its own data in the reflection phase shift in the RIS-SSK-RPM method that has been discussed. The RIS reflection phase can communicate additional RIS information directly in this manner. ka = $log2(Nt)$ and kr = $log2(M)$, respectively, are used to signify the maximum number of information bits that can be delivered through AP and RIS. Additionally, the symbols kr and ka stand for the information bits of RIS and AP, respectively. The presented system can transmit k = ka + kr bits per channel use as a consequence (bpcu). The mapping rule for RIS and AP information bits on reflection phase shift m and TA index I is provided in Table A for M = 2 and Nt = 4.

Table A is showing AP and RIS bit-to-symbol mapping example:

k_a	k_r	$\mathbf{x}$	Phase shift θ	Signal sets
00	0	$\mathbf{a}_1 = [1,0,0,0]^T$	θ_1	$\{\mathbf{a}_1, \theta_1\}$
01	0	$\mathbf{a}_2 = [0,1,0,0]^T$	θ_1	$\{\mathbf{a}_2, \theta_1\}$
11	0	$\mathbf{a}_3 = [0,0,1,0]^T$	θ_1	$\{\mathbf{a}_3, \theta_1\}$
10	0	$\mathbf{a}_4 = [0,0,0,1]^T$	θ_1	$\{\mathbf{a}_4, \theta_1\}$
00	1	$\mathbf{a}_1 = [1,0,0,0]^T$	θ_2	$\{\mathbf{a}_1, \theta_2\}$
01	1	$\mathbf{a}_2 = [0,1,0,0]^T$	θ_2	$\{\mathbf{a}_2, \theta_2\}$
11	1	$\mathbf{a}_3 = [0,0,1,0]^T$	θ_2	$\{\mathbf{a}_3, \theta_2\}$
10	1	$\mathbf{a}_4 = [0,0,0,1]^T$	θ_2	$\{\mathbf{a}_4, \theta_2\}$

If ith TA is turned on at the AP and mth phase shift is employed by the RIS at each specified instant, the received signal at Rx through N reflecting elements can be expressed as follows:

$$\mathbf{Y} = \delta_1\delta_2\sqrt{P_t}\mathbf{G}\Theta\mathbf{H}^T\mathbf{X} + \mathbf{w} = \sqrt{P}\sum_{n=1}^{N} h_{i,n}\mathbf{g}_n \exp\left(j\theta_m\right) + \mathbf{W} \tag{3.1}$$

where $P = \delta_1^2\delta_2^2 P_t$, $\delta 1$ and $\delta 2$ indicate, respectively, the path-losses of the Access Point-to-RIS and RIS-to-

Receiver channels. P_t stands for transmitted power , $\mathbf{Y} \in C^{N_r \times 1}$ is the signal vector at the receiving end, $h_{i,n}$ represents $(i,n)^{th}$ element of H, g_n shows the n^{th} column of G , moreover, the vector of additive white Gaussian noise is $\mathbf{W} \in C^{N_r \times 1}$.
The components of G, H, and W are complex Gaussian random variables (RVs) with independent and identical distributions (i.i.d), zero mean and unity variance.

Let's detect the RPM and SSK symbols simultaneously on the receiver. ML-detector can be provided for eq(3.1) by:

$$\left\{\hat{i}, \theta_{\hat{m}}\right\} = \underset{i,\theta_m}{\operatorname{argmin}} \left\| \mathbf{Y} - \sqrt{P} \sum_{n=1}^{N} h_{i,n} \mathbf{g}_n \exp\left(j\theta_m\right) \right\|^2 \tag{3.2}$$

where, $\hat{i} = 1, 2, \ldots, N_t$ and $\theta_{\hat{m}} \in \theta, \hat{m} = 1, 2, \ldots, M$.
According to the observed transmit antenna (TA) index $\hat{i}$ and phase shift $\theta_{\hat{m}}$, as well as the bits-to-symbol mapping rule displayed in Table A, the bits are mapped to symbols. Rx identifies the data bits that correspond to the observed signal sets, i.e. $a_{\hat{i}}$, $\theta_{\hat{m}}$, where position of the unity element is located in $a_{\hat{i}}$ represents the transmit antenna index $\hat{i}$.

3.4 Performance Analysis

3.4.1 Bit Error Rate Analysis

For finding the bit error rate, we are going to use the term called Pairwise Error Probability (PEP) for the detection of the received signal. The formula for calculating the Conditional Pairwise Error Probability between the sent signal sets $\{i, \theta_m\}$ and detected signal sets $\left\{\hat{i}, \theta_{\hat{m}}\right\}$ is as follows:

$$\text{PEP}\left(\{i, \theta_m\} \rightarrow \left\{\hat{i}, \theta_{\hat{m}}\right\} \mid \mathbf{G}, \mathbf{H}\right) \quad = P_r\left(\left\|\mathbf{Y} - \sqrt{P}\lambda_{i,m}\right\|^2 > \left\|\mathbf{Y} - \sqrt{P}\lambda_{\hat{i},\hat{m}}\right\|^2\right) \tag{3.3}$$

Here,
$\lambda_{i,m} = \sum_{n=1}^{N} h_{i,n}\mathbf{g}_n \exp\left(j\theta_m\right)$ and $\lambda_{\hat{i},\hat{m}} = \sum_{n=1}^{N} h_{\hat{i},n} g_n \exp\left(j\theta_{\hat{m}}\right)$ After putting the values of $\lambda_{i,m}$ and $\lambda_{\hat{i},\hat{m}}$ in eq (3.3), we will have conditional PEP as:

$$\text{PEP}\left(\{i, \theta_m\} \rightarrow \left\{\hat{i}, \theta_{\hat{m}}\right\}\right) = E\left[Q\left(\sqrt{\frac{P}{2}\left\|\lambda_{i,m} - \lambda_{\hat{i},\hat{m}}\right\|^2}\right)\right] \tag{3.4}$$

Now we will prove the eq. 3.4 ;

PROOF I:

$$\mathbf{Y} = \delta_1 \delta_2 \sqrt{P_t} \mathrm{G} \theta H^\top \mathbf{X} + \mathbf{W}$$

$$\mathbf{Y} = \sqrt{P} \sum_{n=1}^{N} h_{i,n} g_n \exp\left(j\theta_m\right) + \mathbf{W}$$

$\lambda_{i,m} = \sum_{n=1}^{N} h_{i,n} g_n \exp\left(\hat{j}\theta_m\right)$

and

$\lambda_{\hat{i},\hat{m}} = \sum_{n=1}^{N} h_{\hat{i},n} g_n \exp(\hat{j}\theta\hat{m})$

$$\Pr\left(\left\|\mathbf{Y} - \sqrt{P}\lambda_{i,m}\right\|^2 > \left\|\mathbf{Y} - \sqrt{P}\lambda_{\hat{i},\hat{m}}\right\|^2\right)$$

$$\Pr\left(\|\mathbf{Y}\|^2 + P\left\|\lambda_{i,m}\right\|^2 - 2\,\mathrm{Re}\left\{\mathbf{Y}^H\sqrt{P}\lambda_{i,m}\right\} > \|\mathbf{Y}\|^2 + P\left\|\lambda_{\hat{i},\hat{m}}\right\|^2 - 2\,\mathrm{Re}\left\{\mathbf{Y}^H\sqrt{P}\lambda_{\hat{i},\hat{m}}\right\}\right)$$

$$\Pr\left(2\sqrt{P}\,\mathrm{Re}\left\{\mathbf{Y}^H\left(\lambda_{i,\hat{m}} - \lambda_{i,m}\right)\right\} > P\left(\|\lambda_{i,\hat{m}}\|^2 - \|\lambda_{i,m}\|^2\right)\right)$$

$$\Pr\left(\mathrm{Re}\left\{\mathbf{Y}^H\left(\lambda_{i,\hat{m}} - \lambda_{i,m}\right)\right\} > \frac{\sqrt{P}}{2}\left(\left\|\lambda_{\hat{i},\hat{m}}\right\|^2 - \|\lambda_{i,m}\|^2\right)\right)$$

Just for convenience:

$\lambda_{\hat{i},\hat{m}} - \lambda_{i,m} = a$

It is assumed that a is given implies that G and H are given. It is given: **W** is Additive White Gaussian Vector with 0 mean and covariance identity matrix.

$$\Pr\left(\mathrm{Re}\left\{\mathbf{Y}^H a\right\} > \frac{\sqrt{P}}{2}\left(\left\|\lambda_{\hat{i},\hat{m}}\right\|^2 - \|\lambda_{i,m}\|^2\right)\right)$$

Let, $\mathbf{W} = \mathbf{Y}^H a = \sum_{i=1}^{n} \mathbf{Y}_i^* a_i$

$E[\mathbf{W}] = \sum_{i=1}^{n} a_i \quad E\left[\mathbf{Y}_i^*\right]$

$E[\mathbf{W}] = \lambda_{i,m}^H a = \sqrt{P}\lambda_{i,m}^H\left(\lambda_{\hat{i},\hat{m}} - \lambda_{i,m}\right)$

$\mathrm{Var}[\mathbf{W}] = \mathrm{Var}\left[\mathbf{Y}^H a\right]$

$\mathrm{Var}[\mathbf{W}] = \sigma^2 I a = \sigma^2 a$

$\mathrm{Var}[\mathbf{W}] = \sigma^2\left\|\hat{\lambda i}, \hat{m} - \lambda_{i,m}\right\|^2$

On RHS we have:

$$\left\|\lambda_{\hat{i},\hat{m}}\right\|^2 - \|\lambda_{i,m}\|^2 = \left(\lambda_{\hat{i},\hat{m}} + \lambda_{i,m}\right)^H\left(\lambda_{\hat{i},\hat{m}} - \lambda_{i,m}\right)$$

$$\Pr\left(\mathrm{Re}(\mathbf{W}) > \frac{\sqrt{P}}{2}\left(\left\|\lambda_{\hat{i},\hat{m}}\right\|^2 - \|\lambda_{i,m}\|^2\right)\right)$$

$$Q\left(\frac{\frac{\sqrt{P}}{2}\left(\left\|\lambda_i,\hat{m}\right\|^2-\left\|\lambda_{i,m}\right\|^2\right)-\sqrt{P}\lambda_{i,m}\,)^H(\lambda_{i,\hat{m}}-\lambda_{i,m})}{\sqrt{\left(\frac{\sigma^2}{2}\right)\left\|\lambda_{i,\hat{m}}-\lambda_{i,m}\right\|^2}}\right) \tag{3.5}$$

As we know, $\sigma^2 = 1$

Now we will solve for numerator:

$$\frac{\sqrt{P}}{2}\left[\left(\lambda_i,\hat{m}+\lambda_{i,m}\right)^H\left(\lambda_{\hat{i}},\hat{m}-\lambda_{i,m}\right)-2\lambda_i^H,m\left(\lambda_{i,\hat{m}}-\lambda_{i,m}\right)\right]$$

$$\frac{\sqrt{P}}{2}\left[\left(\lambda_{\hat{i},\hat{m}}^H-\lambda_{i,m}^H\right)\left(\lambda_{i,\hat{m}}-\lambda_{i,m}\right)\right]$$

$$\frac{\sqrt{P}}{2}\quad\left[\left(\lambda_{\hat{i},\hat{m}}-\lambda_{i,m}\right)^H\left(\lambda_{\hat{i},\hat{m}}-\lambda_{i,m}\right)\right]$$

$$=\frac{\sqrt{P}}{2}\left\|\lambda_{i,\hat{m}}-\lambda_{i,m}\right\|^2 \tag{3.6}$$

On substituting the value of eq. 3.6 in equation eq. 3.5, we get:

$$Q\left(\frac{\frac{\sqrt{P}}{2}\left\|\lambda_{\hat{i}},\hat{m}-\lambda_{i,m}\right\|^2}{\frac{1}{\sqrt{2}}\sqrt{\left\|\lambda_{\hat{i}},\hat{m}-\lambda_{i,m}\right\|^2}}\right)$$

$$Q\left(\sqrt{\frac{P}{2}\left\|\lambda\hat{i},\hat{m}-\lambda_{i,m}\right\|^2}\right)$$

Since condition on G and H is equal to:

$$E\left[\sqrt{\frac{P}{2}\left\|\lambda_{i,m}-\lambda_{i,\hat{m}}\right\|^2}\right]$$

Finally we will have Conditional PEP as:

$$\mathrm{PEP}\left(\{i,\theta_m\}\rightarrow\left\{\hat{i},\theta_{\hat{m}}\right\}\right)=E\left[Q\left(\sqrt{\frac{P}{2}\left\|\lambda_{i,m}-\lambda_{\hat{i},\hat{m}}\right\|^2}\right)\right]$$

where, **Q** represents the q-function of the Gaussian distribution and **E** signifies expectation operation over G and H. By averaging eq. 3.4 over fading channels, it is possible to get the average PEP, which will be used to calculate the ABER of the suggested design.

In addition, the union bound technique for the presented RIS-SSK-RPM method provides a loose ABER bound

in the low SNR domain. Proposition 1 increases the upper limit of ABER for the suggested method.

Theorem 1: The following represents the earlier mentioned bound of Average bit error rate for the suggested method:

ABER $\leq$ ABERSSK + ABERRPM + ABERSSK-RPM,
Where,

$$ABER_{SSK} = \frac{1}{N_t \log_2(N_t M)} \sum_{i=1}^{N_t} \sum_{\hat{i}=1}^{N_t} d_h(i,\hat{i}) \, \mathrm{PEP}(i \to \hat{i}), \tag{3.7}$$

$$ABER_{RPM} = \frac{1}{M \log_2(N_t M)} \sum_{m=1}^{M} \sum_{\hat{m}=1}^{M} d_h(\theta_m, \theta_{\hat{m}}) \, \mathrm{PEP}(\theta_m \to \theta_{\hat{m}}), \tag{3.8}$$

$$\begin{aligned} ABER_{SSK-RPM} =& \frac{1}{N_t M \log_2(N_t M)} \sum_{m=1}^{M} \sum_{i=1}^{N_t} \sum_{\hat{m} \neq m=1}^{M} \sum_{\hat{i} \neq i=1}^{N_t} \Big[d_h(i,\hat{i}) \\ & + d_h(\theta_m, \theta_{\hat{m}}) \Big] \mathrm{PEP}\left(\{i, \theta_m\} \to \left\{ \hat{i}, \theta_{\hat{m}} \right\} \right) \end{aligned} \tag{3.9}$$

The symbol $dh(.,.)$ stands for the Hamming distance between two symbols. $ABER_{RPM}$ represents the possibility of phase shift error when the active transmit antenna index is accurately detected, $ABER_{SSK}$ represents the possibility of transmit antenna index error when phase shift detection is accurate and $ABER_{SSK-RPM}$ indicates the possibility of error when both are erroneously recognised.

Calculation for $PEP(i \to \hat{i})$: In the scenario where the RIS reflects the signal with a m_{th} phase difference, the average PEP over TA indices can be formulated as follows, starting with eq. 3.4:;

$$\mathrm{PEP}(i \to \hat{i}) = \frac{1}{M} \sum_{m=1}^{M} \int_0^{\infty} Q\left(\sqrt{v_m}\right) f(v_m) \, dv_m \tag{3.10}$$

Where, $v_m = \frac{P}{2} \left\| \lambda_{i,m} - \lambda_{\hat{i},\hat{m}} \right\|^2$

Taking into account the "Central Limit Theorem" CLT , vm follows the central "Chi-Square Distribution" with γ is equal to $\frac{PN}{2}$ and s that is 2Nr "Degrees of Freedom". The probability density function of vm could be expressed as follows:

$$f(v_m) = \frac{1}{(2\gamma)^{\frac{s}{2}} \Gamma\left(\frac{s}{2}\right)} v_m^{\frac{s}{2}-1} \exp\left(-\frac{v_m}{2\gamma}\right), v_m > 0 \tag{3.11}$$

Now , we will calculate the mean for v_m:

PROOF II:

$$v_m = \frac{P}{2} \left\| \lambda_{i,m} - \lambda_{i,m} \right\|^2$$

$$v_m = \frac{p}{2} \left\| \sum_{n=1}^{N} h_{i,n} \underline{g}_n e^{j\theta m} - \sum_{n=1}^{N} h_{i,n} \underline{g}_n e^{j\theta m} \right\|^2$$

$$v_m = \frac{P}{2} \left\| \sum_{n=1}^{N} h_{i,n} g_n - h\hat{i}_i, n g_n \right\|^2$$

$$g_n = \begin{bmatrix} g_{1,n} \\ g_{2,n} \\ \vdots \\ g_{Nr,n} \end{bmatrix}_{Nr \times 1}$$

$$g_{r,n}, h_{i,n} \sim CN(0,1)$$

$$h_{i,n} = h_{i,n} + j h_{i,n}$$

$$g_{r,n} = g_{r,n} + j g_{r,n}$$

All the real and imaginary values

$$h_{i,n} * g_n = hi, n \cdot \begin{bmatrix} g_{1,n} \\ g_{2,n} \\ \vdots \\ g_{Nr,n} \end{bmatrix}$$

$$\Rightarrow h_{i,n} * g_{i,n} = (h_{i,n} + j h_{i,n}) \times (g_{r,n} + j g_{r,n})$$

$$= (h_{i,n} g_{r,n} - h_{i,n} g_{r,n}) + \dot{j} \left(h_{i,n} g_{r,n} + h_{i,n} g_{r,n} \right)$$

$$\Rightarrow h\hat{i}, g_{r,n} = \left(h\hat{i}_n \right) + \hat{j} h_{i,n} \Big) \left(g_{r,n} + \hat{j} g_{r,n} \right) = \left(h\hat{i}, n g_{r,n} - h_{i,n} g_{r,n} \right) + \hat{j} \left(h\hat{i}, n g_{r,n} + h_{i,n} g_{r,n} \right)$$

$$= \left(h_{\hat{i},n} g_{r,n} - h_{i,n} g_{r,n} \right) + \hat{j} \left(h_{\hat{i},n} g_{r,n} + h_{i,n} g_{r,n} \right)$$

$$\Rightarrow \sum_{n=1}^{N} h_{i,n} g_n - \sum_{n=1}^{N} h_{\hat{i},n} g_n$$

$$= \begin{bmatrix} \alpha_1 + j\beta_1 \\ \alpha_2 + j\beta_2 \\ \vdots \\ \vdots \\ \alpha_{N\gamma} + j\beta_{N\gamma} \end{bmatrix}_{N\gamma \times 1}$$

$$= \alpha_1^2 + \beta_1^2 + \alpha_2^2 + \beta_2^2 + \cdots + \alpha_{Nr}^2 + \beta_{N_r}^2$$

$$= \left(\alpha_1^2 + \alpha_2^2 + \cdots + \alpha_{N_\gamma}^2\right) + \left(\beta_1^2 + \beta_2^2 + \cdots + \beta_{N_\gamma}^2\right)$$

$$= \mathrm{Nr} + \mathrm{Nr} = 2\mathrm{Nr}$$

At the rth receiver end:

$$\Rightarrow \sum_{n=1}^{N} h_{i,n} g_{r,n} - \sum_{n=1}^{N} h_{\hat{i},n} g_{r,n}$$

$$= \sum_{n=1}^{N} (h_{i,n} g_{r,n} - h_{i,n} - g_{r,n}) - \sum_{n=1}^{N} (h_{i,n} g_{r,n} - h_{i,n} g_{r,n})$$
$$+ j \sum_{n=1}^{N} (h_{i,n} g_{r,n} + h_{i,n} g_{r,n})$$
$$- j \sum_{n=1}^{N} \left(h_{i,n} g_{r,n} + hi,\hat{}ng_{r,n}\right)$$

$$= \alpha_r + j_r \beta_r$$

$$\alpha_\gamma = \sum_{n=1}^{N} \left[h_{i,n} g_{r,n} - h_{i,n} g_{r,n} - h_{\hat{i},n} g_{r,n} + h_{\hat{i},n} g_{r,n}\right]$$

$h_{i,n} g_{r,n}$ is having distribution of 0 mean and 1/4 variance.

$$\Rightarrow E\left[h_{i,n} \cdot g_{r,n}\right] = 0$$

$h_{i,n} \approx k$
$g_{r,n} \approx k$

where $k \in \{r, i\}$

$$\mathrm{Var}[xy] = \mathrm{Var}[x]\,\mathrm{Var}[y] = \tfrac{1}{2} \cdot \tfrac{1}{2} = \tfrac{1}{4}$$

$$\mathrm{Var}\left(\alpha_r\right) = \sum_{h=1}^{N} \tfrac{1}{4} + \tfrac{1}{4} + \tfrac{1}{4} + \tfrac{1}{4}\ \mathrm{Var}\left(\alpha_r\right) = N$$

Now, $\alpha_r \sim \mathcal{N}(0, N)$
$\beta_r \sim \mathcal{N}(0, N)$

As we know, ${\alpha_1}^2 + {\alpha_2}^2 + \cdots + {\alpha_{N_r}}^2 + {\beta_1}^2 + {\beta_2}^2 + \cdots + \beta_{N\gamma}^2$ is equal to 2Nr.

$$\gamma_r = \alpha_r + j\beta_r$$

$\gamma_\gamma \sim \mathcal{N}(0, 2N)$

$\gamma_r = \alpha_\gamma^2 + \beta_r^2 \sim \mathcal{N}(0, N)$

$v_m = \alpha_1^2 + \alpha_2^2 + \cdots \alpha_{N_r}^2 + \beta_1^2 + \beta_2^2 + \cdots + \beta_{N_r}^2$

$E\left[\alpha_i^2\right] = E\left[\beta_i^2\right] = N$

After substituting the value of eq. 3.11 in eq. 3.10 and putting the value of s, we get,

$$PEP(i \to \hat{i}) = \frac{1}{m} \sum_{i=1}^{M} \frac{1}{(2\gamma)^{N_r} \Gamma(N_r)} \int_0^\infty Q\left(\sqrt{v_m}\right) v_m^{Nr-1} \exp\left(\frac{-v_m}{2\gamma}\right) dv_m \tag{3.12}$$

On putting $a = \frac{1}{2\gamma}$, then:

$$\mathrm{PEP}(i \to \hat{i}) = \frac{1}{M} \sum_{i=1}^{M} \frac{(a)^{N_r}}{\Gamma\left(N_r\right)} \int_0^\infty Q\left(\sqrt{v_m}\right) v_m^{(N_r-1)} \exp\left(-a v_m\right) dv_m \tag{3.13}$$

Finding closed form expressions for integrals not listed in the traditional tables of integrals can also be done using the alternative Gaussian Q-function format.[19]
It is given as:

$$J_m(a, b) = \frac{a^m}{\Gamma(m)} \int_0^\infty e^{-at} t^{m-1} Q(\sqrt{bt}) dt \tag{3.14}$$

When m is a positive real number, the previously given equation for this integral exists.Then $J_m(a, b)$ can be shown as:

$$J_m(a, b) = [P(c)]^m \sum_{k=0}^{m-1} \left[\begin{array}{c} m-1+k \\ k \end{array} \right] [1 - P(c)]^k \tag{3.15}$$

where, $P(x) = \frac{1}{2}\left(1 - \sqrt{\frac{x}{1+x}}\right)$,

Since, we can compare eq. 3.13 with eq. 3.14 and write in the form of eq. 3.15 :=

$$\mathrm{PEP}(i \to \hat{i}) = \mu^{N_r} \sum_{j=0}^{N_r-1} \left(\begin{array}{c} N_r - 1 - j \\ j \end{array} \right) [1 - \mu]^j \tag{3.16}$$

where: $\mu = \frac{1}{2}\left(1 - \sqrt{\frac{r}{1+r}}\right)$

Calculation for $\mathrm{PEP}\left(\theta_m \to \theta_{\hat{m}}\right)$:= Additionally, form eq. 3.4 , When the TA index is correctly determined,

it is possible to state that the pairwise error probability between reflection phase changes is:

$$\mathrm{PEP}\left(\theta_m \to \theta_{\hat{m}}\right) = \frac{1}{N_t}\sum_{i=1}^{N_t}\int_0^{\infty} Q\left(\sqrt{\hat{v}_i}\right) f\left(\hat{v}_i\right) d\hat{v}_i \tag{3.17}$$

Where, $\hat{v}_i = \frac{P}{2}\left\|\lambda_{i,m} - \lambda_{i,m}\right\|^2$

$\hat{v}_i = \frac{p}{2}\left\|\sum_{n=1}^{N} h_{i,n}\underline{g}_n e^{j\theta m} - \sum_{n=1}^{N} h_{i,n}\underline{g}_n e^{j\theta_{\hat{m}}}\right\|^2$

The central limit theorem (CLT) is taken into account, $\hat{v}_i$ follows the central Chi-square distribution , and with the similar process that we have done in (PROOF II), we will get the mean of $\hat{v}_i$ like this, $\hat{\gamma} = \frac{PN}{2}\left(1 - \cos\left(\theta_m - \theta_{\hat{m}}\right)\right)$ and s = 2Nr degrees of freedom. The following is a possible way to express the probability density function (PDF) of $\hat{v}_i$:

$$f\left(\hat{v}_i\right) = \frac{1}{(2\gamma)^{\frac{s}{2}}\Gamma\left(\frac{s}{2}\right)}\hat{v}_i^{\frac{s}{2}-1}\exp\left(-\frac{\hat{v}_i}{2\gamma}\right), v_m > 0 \tag{3.18}$$

After substituting the value of eq. 3.18 in eq. 3.17 and putting the value of s, we get,

$$PEP(\theta m \to \theta\hat{m}) = \frac{1}{N_t}\sum_{i=1}^{N_t}\frac{1}{(2\gamma)^{N_r}\Gamma(N_r)}\int_0^{\infty} Q\left(\sqrt{\hat{v}_i}\right)\hat{v}_i^{Nr-1}\exp\left(\frac{-\hat{v}_i}{2\gamma}\right) d\hat{v}_i \tag{3.19}$$

On putting $a = \frac{1}{2\gamma}$, then:

$$\mathrm{PEP}(\theta m \to \theta\hat{m}) = \frac{1}{N_t}\sum_{i=1}^{N_t}\frac{(a)^{N_r}}{\Gamma\left(N_r\right)}\int_0^{\infty} Q\left(\sqrt{\hat{v}_i}\right)\hat{v}_i^{(N_r-1)}\exp\left(-a\hat{v}_i\right) d\hat{v}_i \tag{3.20}$$

Since, we can compare eq. 3.20 with eq. 3.14 and write in the form of eq. 3.15:=

$$\mathrm{PEP}\left(\theta_m \to \hat{\theta}_m\right) = \tilde{\mu}^{N_r}\sum_{j=0}^{N_r-1}\begin{pmatrix} N_r - 1 - j \\ j \end{pmatrix}[1-\hat{\mu}]^j \tag{3.21}$$

hence, $\tilde{\mu} = \frac{1}{2}\left[1 - \sqrt{\left(\frac{\tilde{\gamma}}{1+\tilde{\gamma}}\right)}\right]$

Calculation for $\mathrm{PEP}\left(\{i,\theta_m\} \to \left\{\hat{i},\theta_{\hat{m}}\right\}\right)$

Furthermore, using eq (3.4), The combined Pairwise Probability between two entities can be ascertained:

$$\mathrm{PEP}\left(\{i,\theta_m\} \to \left\{\hat{i},\theta_{\hat{m}}\right\}\right) = \int_0^{\infty} Q(\sqrt{\tilde{v}})f(\tilde{v})d\tilde{v} \tag{3.22}$$

$\tilde{v}_i = \frac{P}{2}\left\|\lambda_{i,m} - \lambda_{\hat{i},\hat{m}}\right\|^2$

$\tilde{v}_i = \frac{p}{2}\left\|\sum_{n=1}^{N} h_{i,n}\underline{g}_n e^{j\theta m} - \sum_{n=1}^{N} h_{\hat{i},n}\underline{g}_n e^{j\theta_{\hat{m}}}\right\|^2$

The central limit theorem (CLT) is taken into account, and $\tilde{v}$ follows the same distribution as mentioned in earlier equations and with the similar process that we have done in (PROOF II), we will get the mean of $\tilde{v}_i$ like this $\tilde{\gamma} = \frac{PN}{2}$ and s = 2Nr degrees of freedom. The following is a possible way to express the probability density function (PDF) of $\tilde{v}$:

$$f(\tilde{v}) = \frac{1}{(2\tilde{\gamma})^{\frac{s}{2}}\Gamma\left(\frac{s}{2}\right)} \tilde{v}^{\frac{s}{2}-1} \exp\left(-\frac{\tilde{v}}{2\tilde{\gamma}}\right), \tilde{v} > 0 \tag{3.23}$$

After substituting the value of eq. 3.23 in eq. 3.22 and putting the value of s, we get,

$$PEP\left(\{i,\theta_m\} \to \left\{\hat{i},\theta_{\hat{m}}\right\}\right) = \frac{1}{N_t}\sum_{i=1}^{N_t} \frac{1}{(2\gamma)^{N_r}\Gamma(N_r)} \int_0^{\infty} Q\left(\sqrt{\tilde{v}_i}\right) \tilde{v}_i^{Nr-1} \exp\left(\frac{-\tilde{v}_i}{2\gamma}\right) d\tilde{v}_i \tag{3.24}$$

Since, we can compare eq. 3.24 with eq. 3.14 and write in the form of eq. 3.15:=

$$\text{PEP}\left(\{i,\theta_m\} \to \left\{\hat{i},\theta_{\hat{m}}\right\}\right) = \tilde{\mu}_{N_r} \sum_{j=0}^{N_r-1} \begin{pmatrix} N_r-1-j \\ j \end{pmatrix} [1-\tilde{\mu}]^j \tag{3.25}$$

where, $\tilde{\mu} = \frac{1}{2}\left[1 - \sqrt{\left(\frac{\tilde{\gamma}}{1+\tilde{\gamma}}\right)}\right]$

Understanding of Hamming Distance: This is one possible way to $d_h\left[\{i,\theta_m\}, \left\{\hat{i},\theta_{\hat{m}}\right\}\right]$ to represent the mentioned distance over the sent signal sets i,θ_m and $\hat{i},\theta_{\hat{m}}$. . When error bits are present at Rx, there are three possible scenarios. In the following scenarios (i) "Transmit Index" is identified improperly (ii) RIS phase difference is not correctly identified at this time.(iii) or both identified in an improper manner.
In addition, the distance that has been mentioned can be represented:
$d_h\left[\{i,\theta_m\}, \left\{\hat{i},\theta_{\hat{m}}\right\}\right] = d_h(i,\hat{i}) + d_h(\theta_m,\theta_{\hat{m}})$

where, In **Theorem 1** these parameters are used.
Additionally, the following provides evidence for Theorem 1:

1. Only when the proper detection of phase shift θm at Rx takes place does the $ABER_{SSK}$ occur. In this situation, we note the following: $d_h(\theta_m,\theta_{\hat{m}})$ and $PEP\left(\{i,\theta_m\} \to \left\{\hat{i},\theta_{\hat{m}}\right\}\right)$ is comparable to $PEP(i \to \hat{i})$.

2. Taking into account all of the terms for which i is equal to $\hat{i}$ and m is not equal to $\hat{m}$ the ABE_{RRPM} may be found from eq. 3.4. In this instance, we observe that: $d_h(i,\hat{i})$ is equal to zero and $PEP\left(\{i,\theta_m\}\right.$ tends to $\left\{\hat{i},\theta_{\hat{m}}\right\}$ is comparable to $PEP(\theta m \to \hat{\theta m})$.

3. All terms for which neither $i = \hat{i}$ nor $m = \hat{m}$ are collected by the $ABER_{SSK-RPM}$. In this instance, it is evident that: $d_h(i \to \hat{i})$ is not equal to 0, $d_h\left(\theta_m \to \theta_{\hat{m}}\right)$ is not equal to 0, and PEP is comparable to $PEP(\theta m \to \hat{\theta m})$.

3.4.2 Diversity Analysis

The $ABER_{SSK-RPM}$ is larger than the $ABER_{RPM}$ and $ABER_{SSK}$, as can be seen from eq. 3.9 . As a result, in the high SNR zone, system ABER is similar to $ABER_{SSK-RPM}$. Furthermore, we may obtain $\text{PEP}\left(\{i,\theta_m\} \rightarrow \left\{\hat{i},\theta_{\hat{m}}\right\}\right)$ at high SNR since $ABER_{SSK-RPM}$ is related to the specified probability.

Now, we will prove that $\text{PEP}\left(\{i,\theta_m\} \rightarrow \left\{\hat{i}_1,\theta_{\hat{m}}\right\}\right) = \frac{1}{2}\left(\frac{1}{1+\tilde{\gamma}}\right)^{N_r}$:

PROOF III

We use the Chernov bound for eq. 3.22 to find the diversity order.

$$\text{PEP}\left(\{i,\theta_m\} \rightarrow \left\{\hat{i},\theta_{\hat{m}}\right\}\right) = \int_0^{\infty} Q(\sqrt{\tilde{v}}) f(\tilde{v}) d\tilde{v} \tag{3.26}$$

and from eq. 4.23 , we have: $f\left(\tilde{v}\right) = \frac{1}{(2\gamma)^{\frac{s}{2}}\Gamma\left(\frac{s}{2}\right)} \tilde{v}^{\frac{s}{2}-1} \exp\left(-\frac{\tilde{v}}{2\gamma}\right), \tilde{v} > 0$

Chernov bound is given as:

$$Q(x) \leq \frac{1}{2}\exp\left(-\frac{x^2}{2}\right) \tag{3.27}$$

when we put the value of $\tilde{v}$ in the eq. 3.27 , we get;

$$Q(\sqrt{\tilde{v}}) \leq \frac{1}{2}\exp\left(-\frac{\tilde{v}^2}{2}\right) \tag{3.28}$$

After putting the value of s=Nr , $f\left(\tilde{v}\right)$ and eq. 3.26 , we get;

$$\text{PEP}\left\{\{i,\theta_m\} \rightarrow \left\{\hat{i}_1,\hat{m}\right\}\right) = \frac{1}{2^{Nr+1}\tilde{\gamma}^{N_r}\Gamma\left(N_r\right)} \int_0^{\infty} \tilde{v}_{\gamma}^{N_r-1} \exp^{-\tilde{v}} \left(\frac{1}{2\tilde{\gamma}} + \frac{1}{2}\right) d\tilde{v} \tag{3.29}$$

Now, we will solve this integration with the help of gamma function , which is given by:

$$\text{Put,} \quad \int_0^{\infty} t^{z-1} e^{-t} dt \tag{3.30}$$

Let, $\tilde{v}\left(\frac{1}{2\tilde{\gamma}} + \frac{1}{2}\right) = y$

After differentiating this term, we get;

$d\tilde{v}\left(\frac{1}{2\tilde{\gamma}} + \frac{1}{2}\right) = dy$

After putting these values in the integration part of eq. 3.29 , we get;

$$\Rightarrow \int_0^{\infty} e^{-y} \left(\frac{y}{\frac{1}{2\tilde{r}} + \frac{1}{2}}\right)^{Nr-1} \frac{dy}{\left(\frac{1}{2\tilde{r}} + \frac{1}{2}\right)} \tag{3.31}$$

$$\Rightarrow \frac{1}{\left(\frac{1}{2\tilde{r}}+\frac{1}{2}\right)^{Nr}}\int_0^{\infty} e^{-y}y^{(Nr-1)}dy \tag{3.32}$$

Now, by using eq(3.30), we have;

$$\int_0^{\infty} e^{-y}y^{(Nr-1)}dy = \Gamma(Nr) \tag{3.33}$$

After putting the value of eq. 3.33 in eq. 3.29 , we have;

$$\mathrm{P}\varepsilon\mathrm{p}\left(\{i,\theta_m\},\left\{\hat{i}_1,\hat{\theta}\right\}\right) = \frac{1}{2^{Nr+1}\tilde{r}^{Nr}} \times \frac{1}{\left(\frac{1}{2\tilde{r}}+\frac{1}{2}\right)^{Nr}} \tag{3.34}$$

After doing some algebric calculations in eq. 3.34 , we get;

$$\mathrm{PEP}\left(\{i,\theta_m\} \rightarrow \left\{\hat{i}_1,\theta_{\hat{m}}\right\}\right) = \frac{1}{2}\left(\frac{1}{1+\tilde{\gamma}}\right)^{N_r} \tag{3.35}$$

when we put the value of mean i.e. $\tilde{\gamma} = \frac{PN}{2}$;

$$\mathrm{PEP}\left(\{i,\theta_m\} \rightarrow \{\hat{i},\theta_{\hat{m}}\}\right) = \left(\frac{2}{PN}\right)^{N_r} \tag{3.36}$$

From equation 3.36, it is clear that the coding advantage is $\frac{N}{2}$.

3.4.3 Ergodic Capacity Analysis

The EC is the term used to describe the median capacity over fading channels. In the suggested technique, the information bits are sent using discrete constellations. As a result, we examine the discrete-input continuous-output memory-less channel (DCMC) capacity, which is denoted by the expression below:

$$C = E\left[\max I(\mathbf{z},\theta;\mathbf{y})\right] \tag{3.37}$$

Now, We will prove that $C = 2\log_2\left(N_tM\right) - \log_2\left[N_tM + \sum_{m=1}^{M}\sum_{i=1}^{N_t}\sum_{\hat{m}\neq m=1}^{M}\sum_{i\neq i=1}^{N_t}\Psi_{\alpha}(\gamma)\right]$

PROOF IV

Here, $I(\mathbf{z},\theta;\mathbf{y})$ is the mutual information between the receiving vector y and the input signal sets.
According to the chain rule, the mentioned information is given by:

$$I(\mathbf{z},\theta;\mathbf{y}) = I(\theta;\mathbf{y}) + I(\mathbf{z};\mathbf{y}\mid\theta) \tag{3.38}$$

where, first term tells about θ and second term shows the sum of information y tells about z for a defined θ.
Further $I(\theta;\mathbf{y})$ defined as:

$$I(\theta;\mathbf{y}) = \underbrace{\sum_{\theta}\int_{\mathbf{y}} f(\theta)f(\mathbf{y}\mid\theta)\log_2 f(\mathbf{y}\mid\theta)d\mathbf{y}}_{\alpha_1} - \underbrace{\sum_{\theta}\int_{\mathbf{y}} f(\theta)f(\mathbf{y}\mid\theta)\log_2 f(\mathbf{y})d\mathbf{y}}_{\alpha_2} \tag{3.39}$$

The conditional PDF is represented by $f(*|*)$. Additionally, $I(\mathbf{z};\mathbf{y} \mid \theta)$ can be calculated as:

$$I(\mathbf{z};\mathbf{y} \mid \theta) = \underbrace{\sum_{\theta}\sum_{\mathbf{z}}\int_{\mathbf{y}} f(\mathbf{z},\mathbf{y} \mid \theta)\log_2 f(\mathbf{y} \mid \mathbf{z},\theta)d\mathbf{y}}_{\beta_1} - \underbrace{\sum_{\theta}\sum_{\mathbf{z}}\int_{\mathbf{y}} f(\mathbf{z},\mathbf{y} \mid \theta)\log_2 f(\mathbf{y} \mid \theta)d\mathbf{y}}_{\beta_2} \tag{3.40}$$

The terms α_1 and β_2 will be equivalent when the conditional PDFs of y have been substituted, as can be seen from eq. 3.39 and eq. 3.40. In light of this, from eq (3.38) to eq (3.40), the proposed the terms α_2 and β_1 will work as a scheme. The reciprocal information for the suggested scheme is expressed as:

$$I(\mathbf{z},\theta;\mathbf{y}) = \beta_1 - \alpha_2 \tag{3.41}$$

where the expression β_1 refers to the entropy of the noise vector w: [20]

$$\beta_1 = -N_r \log_2(\pi \exp(1)) \tag{3.42}$$

By eq. 3.39, α_2 can be defined:

$$\alpha_2 = \sum_{m=1}^{M}\int_{C^{N_r}} f\left(\theta=\theta_m\right) f\left(\mathbf{y} \mid \theta=\theta_m\right)\log_2 f(\mathbf{y})d\mathbf{y} \tag{3.43}$$

eq. 3.38 and eq. 3.39 can be used to lower bound α_2 as;

$$\alpha_2 \geq \log_2\left[\sum_{m=1}^{M}\int_{C^{N_r}} f\left(\theta=\theta_m\right) f\left(\mathbf{y} \mid \theta=\theta_m\right) f(\mathbf{y})\right] d\mathbf{y} \tag{3.44}$$

The probabilities of choosing the ith transmit antenna and the mth phase shift at once are $f(hi) = \frac{1}{N_t}$ and $f(m) = \frac{1}{m}$, respectively. The PDF of y can be calculated as:

$$f(\mathbf{y}) = \frac{1}{N_t M}\sum_{i=1}^{N_t}\sum_{m=1}^{M}\frac{1}{\pi^{N_r}}\exp\left(-\left\|\mathbf{y}-\sqrt{P}\lambda_{i,m}\right\|^2\right) \tag{3.45}$$

moreover, y's conditional PDF should be;

$$f\left(\mathbf{y} \mid \theta=\theta_m\right) = \frac{1}{N_t}\sum_{i=0}^{N_t}\frac{1}{\pi^{N_r}}\exp\left(-\left\|\mathbf{y}-\sqrt{P}\lambda_{i,m}\right\|^2\right) \tag{3.46}$$

On putting the value of eq. 3.45 and eq. 3.46 in eq. 3.43 ;

$$\alpha_2 \geq \log_2\left(\frac{\sum_{i=1}^{N_t}\sum_{m=1}^{M}\sum_{\hat{m}=1}^{M}\sum_{\hat{i}=1}^{N_t}\exp\left(-\frac{P}{2}\left\|\lambda_{i,m}-\lambda_{\hat{i},\hat{m}}\right\|^2\right)}{(2\pi)^{N_r}\left(N_t M\right)^2}\right) \tag{3.47}$$

On putting the values of eq. 3.47 and eq. 3.42 into eq. 3.41 , we get;

$$I(\mathbf{z},\theta;\mathbf{y}) \approx 2\log_2\left(N_t M\right) - \log_2\left[N_t M + \sum_{i=1}^{N_t}\sum_{m=1}^{M}\sum_{\hat{m}\neq m=1}^{M}\sum_{\hat{i}\neq i=1}^{N_t} \times E\left[\exp\left(-\frac{P}{2}\left\|\lambda_{i,m}-\lambda_{\hat{i},\hat{m}}\right\|^2\right)\right]\right] \tag{3.48}$$

$\psi_\alpha(\gamma) = E[\exp(-\gamma\alpha)]$ and $\gamma = \frac{P}{2}$

where,

$\alpha = \frac{P}{2}\left\|\lambda_{i,m} - \lambda_{\hat{i},\hat{m}}\right\|^2$

$\alpha = \frac{p}{2}\left\|\sum_{n=1}^{N} h_{i,n}\underline{g}_n e^{j\theta m} - \sum_{n=1}^{N} h_{\hat{i},n}\underline{g}_n e^{j\theta \hat{m}}\right\|^2$

Keep in mind that, the elements of the channel matrices H and G follow the chi-square distribution, with mean 'N' and '2Nr' degrees of freedom, and their moment generating function is generated by independent RVs that are identically distributed;

$$\psi_\alpha(\gamma) = \left(\frac{1}{1+2N_r}\right)^{N_r} \tag{3.49}$$

Last but not least, by inserting eq. 3.49 into eq. 3.48 and taking into account the fact that for discrete input, I (x, y) maximises for equally likely inputs, we get eq. 3.50 ;

$$C = 2\log_2(N_t M) - \log_2\left[N_t M + \sum_{m=1}^{M}\sum_{i=1}^{N_t}\sum_{\hat{m}\neq m=1}^{M}\sum_{i\neq i=1}^{N_t}\Psi_\alpha(\gamma)\right] \tag{3.50}$$

CHAPTER 4
Conclusion and Future Work

4.1 Conclusion

We have explored into such a revolutionary **RIS-SSK-RPM** scheme that makes use of the advantages of both a **RIS** and an **SSK** to their fullest extent. The suggested method explicitly transmits the information via reflection phase shift while reflecting the incoming Radio Frequency (RF) signal, increasing the communication connection dependability and Spectral Efficiency (SE) of the system. A closed-form expression of average pairwise error probability (PEP) over fading channels has also been developed under the assumption of Maximum Likelihood (ML) detection, and it is utilised to assess the unified tight upper bound expression of ABER for the suggested scheme. Additionally, a new paradigm for ergodic capacity (EC) analysis and diversity analysis has been presented.

4.2 Future Work

Extensive Monte Carlo simulation results will be used to confirm all the theoretically verified outcomes. We will focus more on the reflection phase modulation (RPS) and intelligent reflecting surface-assisted space shift keying (SSK) modulation techniques. We will carry out the combined identification of SSK and RPM symbols using the best detection method for an outdated channel environment scenario with channel estimate error.

Note: I would especially want to thank my supervisor for providing me the **Proof I** and **Proof II** solutions so that I could go on and calculate eq(3.3) and eq(3.10), respectively.

Bibliography

[1] R. Mesleh, S. S. Ikki, E.-H. M. Aggoune, and A. Mansour, "Performance analysis of space shift keying (ssk) modulation with multiple cooperative relays," *EURASIP Journal on Advances in Signal Processing*, vol. 2012, no. 1, pp. 1–10, 2012.

[2] J. F. A. Rida, "Overview of development performance for mobile phone wireless communication networks," in *2021 International Conference on Electrical, Computer and Energy Technologies (ICECET)*, 2021, pp. 1–11.

[3] E. Basar, M. Di Renzo, J. De Rosny, M. Debbah, M.-S. Alouini, and R. Zhang, "Wireless communications through reconfigurable intelligent surfaces," *IEEE Access*, vol. 7, pp. 116 753–116 773, 2019.

[4] X. Wei, D. Shen, and L. Dai, "Channel estimation for ris assisted wireless communications—part i: Fundamentals, solutions, and future opportunities," *IEEE Communications Letters*, vol. 25, no. 5, pp. 1398–1402, 2021.

[5] Y. Chau and S.-H. Yu, "Space modulation on wireless fading channels," in *IEEE 54th Vehicular Technology Conference. VTC Fall 2001. Proceedings (Cat. No.01CH37211)*, vol. 3, 2001, pp. 1668–1671 vol.3.

[6] N. Rajatheva, I. Atzeni, S. Bicais, E. Bjornson, A. Bourdoux, S. Buzzi, C. D'Andrea, J.-B. Dore, S. Erkucuk, M. Fuentes *et al.*, "Scoring the terabit/s goal: Broadband connectivity in 6g," *arXiv preprint arXiv:2008.07220*, 2020.

[7] F. Boccardi, R. W. Heath, A. Lozano, T. L. Marzetta, and P. Popovski, "Five disruptive technology directions for 5g," *IEEE Communications Magazine*, vol. 52, no. 2, pp. 74–80, 2014.

[8] Q. Wu, G. Y. Li, W. Chen, D. W. K. Ng, and R. Schober, "An overview of sustainable green 5g networks," *IEEE Wireless Communications*, vol. 24, no. 4, pp. 72–80, 2017.

[9] Q. Wu and R. Zhang, "Intelligent reflecting surface enhanced wireless network via joint active and passive beamforming," *IEEE Transactions on Wireless Communications*, vol. 18, no. 11, pp. 5394–5409, 2019.

[10] Q. Wu, S. Zhang, B. Zheng, C. You, and R. Zhang, "Intelligent reflecting surface-aided wireless communications: A tutorial," *IEEE Transactions on Communications*, vol. 69, no. 5, pp. 3313–3351, 2021.

[11] S. B. Patel, D. V. Chauhan, and J. D. Patel, "Spatial modulation: Challenges and potential solutions," in *2021 International Conference on Smart Generation Computing, Communication and Networking (SMART GENCON)*, 2021, pp. 1–8.

[12] U. Singh, M. R. Bhatnagar, and T. A. Tsiftsis, "Feedback-based ssk modulation: Constellation design and performance results," *IEEE Transactions on Communications*, vol. 68, no. 11, pp. 6902–6917, 2020.

[13] P. Modepalli and S. Lakshmi, "Survey on multiple antenna techniques to improve spectral efficiency with minimum rf chains," in *2019 IEEE International Conference on Electrical, Computer and Communication Technologies (ICECCT)*, 2019, pp. 1–4.

[14] X. Tan, Z. Sun, J. M. Jornet, and D. Pados, "Increasing indoor spectrum sharing capacity using smart reflect-array," in *2016 IEEE International Conference on Communications (ICC)*, 2016, pp. 1–6.

[15] L. Subrt and P. Pechac, "Controlling propagation environments using intelligent walls," in *2012 6th European Conference on Antennas and Propagation (EUCAP)*, 2012, pp. 1–5.

[16] E. Basar, "Reconfigurable intelligent surface-based index modulation: A new beyond mimo paradigm for 6g," *IEEE Transactions on Communications*, vol. 68, no. 5, pp. 3187–3196, 2020.

[17] A. E. Canbilen, E. Basar, and S. S. Ikki, "Reconfigurable intelligent surface-assisted space shift keying," *IEEE Wireless Communications Letters*, vol. 9, no. 9, pp. 1495–1499, 2020.

[18] U. Singh, M. R. Bhatnagar, and A. Bansal, "Ris-assisted ssk modulation: Reflection phase modulation and performance analysis," *IEEE Communications Letters*, vol. 26, no. 5, pp. 1012–1016, 2022.

[19] M.-S. Alouini and A. Goldsmith, "A unified approach for calculating error rates of linearly modulated signals over generalized fading channels," *IEEE Transactions on Communications*, vol. 47, no. 9, pp. 1324–1334, 1999.

[20] U. Singh, M. R. Bhatnagar, and J. Nebhen, "Quadrature spatial modulation-assisted full-duplex communication," *IEEE Wireless Communications Letters*, vol. 10, no. 12, pp. 2629–2633, 2021.